Machine Learning-Driven Framework for Reducing PAPR in Satellite Communication Systems

Carla E. Garcia[1], Francisco J. Martin Vega[2], Mario R. Camana[1], Jorge Querol[1], Saud Althunibat[3], Khalid Qaraqe[4], and Symeon Chatzinotas[1]
[1]Interdisciplinary Centre for Security, Reliability and Trust (SnT), University of Luxembourg, Luxembourg City, Luxembourg
[2]University of Malaga, Malaga, Spain
[3] Department of Communication Engineering, Al-Hussein Bin Talal University, Ma'an 23874, Jordan
[4]College of Science and Engineering, Hamad Bin Khalifa University, Doha, Qatar
Emails: carla.garcia@uni.lu, fjmv@uma.es, {mario.camana, jorge.querol}@uni.lu,
saud.althunibat@ahu.edu.jo, kqaraqe@hbku.edu.qa, symeon.chatzinotas@uni.lu.

***Abstract*—High peak-to-average power ratio (PAPR) in orthogonal frequency division multiplexing (OFDM) signals presents a persistent challenge in satellite communications (SatCom), impacting signal quality and causing adjacent channel interference. This paper introduces a novel framework that combines the elastic net-based machine learning (ML) model with the partial transmit sequence (PTS) technique to effectively reduce PAPR. Additionally, the potential of artificial intelligence (AI) approaches are investigated, specifically swarm intelligence and ML methods, for high-performance, low-complexity solutions. In this regard, ML models are applied to mitigate PAPR in SatCom networks under the presence of a traveling wave tube amplifier (TWTA) model and a land mobile satellite (LMS) channel, employing 16-quadrature amplitude modulation (16-QAM). Compared with the baseline schemes, simulation results demonstrate that the proposed ML framework, integrating principal component analysis (PCA) with the elastic net learning model, achieves comparable PAPR performance and minimal computational complexity.**

***Index Terms*—Satellite communication system (SatCom), land mobile satellite (LMS), peak-to-average power ratio (PAPR), machine learning (ML), swarm intelligence, partial transmit sequence (PTS).**

I. Introduction

Satellite communication (SatCom) systems encounters significant challenges at the physical layer due to impairments like non-linearity and out-of-band emissions (OBEs), especially when integrating satellite systems with terrestrial networks (TNs). As part of ongoing 3GPP standardization efforts, Orthogonal Frequency Division Multiplexing (OFDM) waveforms, which were originally developed for TNs, are considered for satellite integration. However, OFDM encounters limitations in satellite systems, notably peak-to-average power ratio (PAPR) and adjacent channel interference (ACI) issues, largely stemming from the non-linear behavior of high-power amplifiers (HPAs) [1]. To address these limitations, the partial transmit sequence (PTS) technique has emerged as a promising solution for mitigating high PAPR in SatCom by efficiently combining signal subblocks [1], [2]. One main advantage of PTS is that it is a distortionless approach, utilizing signal scrambling to reduce PAPR without altering signal integrity. As a probabilistic method, PTS also outperforms other probabilistic approaches, such as selected mapping (SLM) and interleaving techniques, in PAPR reduction effectiveness [2].

Among artificial intelligence (AI) architectures, researchers have investigated both swarm intelligence algorithms (SIA) and machine learning (ML) models to deal with PAPR reduction and manage computational complexity (CC). For instance, in [3], the authors applied a particle swarm optimization (PSO)-assisted PTS scheme to lower PAPR, demonstrating that increasing the number of particles enhances the complementary cumulative distribution function (CCDF) performance. Similarly, in [4], the authors compared various swarm intelligence methods, including artificial bee colony (ABC), ant colony optimization (ACO), gray wolf optimization (GWO), genetic algorithm (GA), and PSO, to identify the optimal algorithm for PAPR reduction. Their results indicated that ACO acchieved a superior CCDF performance. On the other hand, regarding ML-based approaches, [5] and [6] proposed a deep learning-based framework for PAPR reduction in OFDM systems, achieving comparable CCDF performance with lower complexity. In [5], the authors integrated the conventional PTS technique with a forward neural network (FNN)-based ML model to reduce PAPR. The authors highlighted that the PTS-FNN method achieved a 32.4% reduction in CC compared to the conventional PTS approach, while also providing significant PAPR reduction.

Accordingly, motivated by the flexible learning ability of the SIA and the ML-based scheme, we investigate three SIA and four ML schemes aided PTS technique to reduce the PAPR in the subsequent subsection. Overall, SIAs rely on particles

This work was supported by the European Space Agency (ESA) under Contract No. 4000130962/20/NL/NL/FE for the project "Satellite Communications with AI-OFDM Waveform for PAPR and ACI Reduction (SAFARI)." This research also was supported in part by the project sElf-evolving terrestrial/nonTerrestrial Hybrid nEtwoRks (ETHER). The ETHER Project was supported by the Smart Networks and Services Joint Undertaking (SNS JU) through the European Union's Horizon Europe Research and Innovation Programme under Grant 101096526. Additional support was provided by the Qatar Research, Development and Innovation (QRDI) Fund—part of Qatar Foundation—through grant NPRP14C-0909-210008.

that iteratively update to converge toward an optimal solution. Meanwhile, the ML techniques employ training models on datasets to identify patterns within data, enabling predictive insights. In this paper, we use the following SIAs: PSO, ACO, and the quantum particle swarm optimization (QPSO) [7]. On the other hand, the ML schemes are the extra randomized tree regressor (ERTR), the random forest (RF), the support vector regressor (SVR), and the elastic net (EN) algorithms [8], [9]. To the best of our knowledge, none of the aforementioned works have considered the implementation of a SAI-aided PTS-based scheme neither ML-based framework in an end-to-end SatCom system for the PAPR analysis. In addition, we performed a comparison between the SIA and the ML-base schemes in terms of PAPR reduction, computational time (CT), and CC. The case of the optimal exhaustive search (ES) method is also considered as a bound on PAPR reduction with the highest CT and CC. Here, ES refers to the standard PTS scheme without the application of any AI algorithm, i.e., the search for the optimal phase factor is performed in an exhaustive search manner.

II. System Model

In this section, we describe the proposed end-to-end SatCom system, which utilizes OFDM waveforms transmitted through a nonlinear channel that considers the impact of a non-ideal high power amplifier (HPA) and a multi-path land mobile satellite (LMS) channel. The proposed system incorporates an ML-aided PTS framework to address the high PAPR in OFDM, as illustrated in Fig. 1. Additionally, we implemented swarm intelligence-based algorithms, instead of the ML framework, as a baseline for comparison. At the transmitter, the bit stream is encoded using a Low-Density Parity-Check (LDPC) encoder based on the belief propagation technique. The encoded bits are then mapped to constellation points using 16-quadrature amplitude modulation (QAM) with a code rate equal to $Rt = 616/1024$, which is specified in the 3GPP 5G standard. Then, the resulting 16-QAM symbols are organized into a resource grid, denoted as $\mathbf{X}_{\mathrm{RG}} \in \mathbb{C}^{M\times S}$, where M represents the number of subcarriers and S indicates the number of symbols. This resource grid provides a structured layout for arranging symbols prior to transmission. Additionally, reference signals known as pilot symbols are inserted at strategic positions within the grid. These pilot symbols are for enabling accurate channel estimation at the receiver.

The conventional PTS method functions by dividing the input data block into equal-sized subblocks [2]. In this context, each column of the resource grid (RG) $\mathbf{X}_{\mathrm{RG}}$ is treated as an input data block, denoted as X, which is segmented into non-overlapping subblocks X_v for $v = \{1, 2, \ldots, V\}$, where V represents the number of subblocks. Each subblock is then transformed from the frequency domain to the time domain using the inverse Discrete Fourier Transform (IDFT).

$$x_v[m] = \sum_{k=0}^{M-1} X_v[k] e^{j2\pi mk/M}, \tag{1}$$

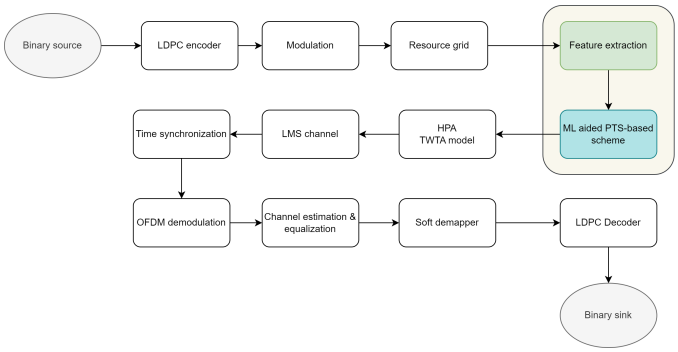

Fig. 1. Diagram block of an OFDM system with the swarm intelligence aided the PTS technique.

where $0 \leq m \leq M-1$ and $X_v[k]$ denotes the symbol on the k-th subcarrier. Te reduce the PAPR of the combined time-domain signal, each subblock $x_v[m]$ is multiplied by a corresponding phase weighting factor vector W_v. The resulting signal, denoted as $x[m]$, is defined as the sum of these modified subblocks,

$$x[m] = \sum_{v=1}^{V} W_v x_v[m]. \tag{2}$$

The PAPR of the combined signal $x[m]$ is then defined as

$$\mathrm{PAPR}(x[m]) = \frac{\max\limits_{0\leq m\leq M-1} |x[m]|^2}{\mathbb{E}\{|x[m]|^2\}}, \tag{3}$$

where the denominator is the average power of $x[m]$. The modified sub-blocks together create a set of candidate signals, from which the signal with the lowest PAPR value is selected for transmission. Moreover, to facilitate accurate data recovery at the receiver, the index of the optimal phase factor that minimizes the PAPR must be sent as side information. This index acts as a reference, enabling the receiver to reconstruct the transmitted signal with the appropriate phase adjustment.

According to the block diagram shown in Fig. 1, before transmitting the signal with the lowest PAPR, it first passes through a HPA. The input signal to the HPA is represented as $r(t) = |r(t)|e^{j\phi(t)}$, where $|r(t)|$ and $\phi(t)$ denotes the amplitude and phase of the input signal, respectively. Then, the output of the HPA can be expressed as $y(t) = G[|r(t)|]e^{j\{\phi(t)+\Phi[|r(t)|]\}}$, where $G[\cdot]$ and $\Phi[\cdot]$ represent the amplitude/amplitude (AM/AM) and amplitude/phase (AM/PM) conversions, respectively. These conversions characterize the nonlinear effects on the amplitude $|r(t)|$ and phase $\phi[\cdot]$ of the input signal. We employ the traveling wave tube Aamplifier (TWTA) model to represent the behavior of the HPA [10], which is characterized by the following expressions:

$$G[|r(t)|] = \frac{\alpha_a |r(t)|}{(1+\beta_a)|r(t)|^2}, \tag{4}$$

and

$$\Phi[|r(t)|] = \frac{\alpha_\phi |r(t)|^2}{(1+\beta_\phi)|r(t)|^2}, \tag{5}$$

where α_a, β_a, α_ϕ, and β_ϕ are parameters that control the characteristics of AM/AM and AM/PM conversions. We utilize the parameters established in [10], which are based on empirical measurements and characterize the performance of the TWTA under specific operational conditions.

The amplified signal is sent through the LMS channel, where it experiences distortion and attenuation. Upon reaching the receiver, the received OFDM signal is demodulated using the Fast Fourier Transform (FFT), aided by pilot symbols for channel estimation. The data symbols are equalized according to the estimated channel response and then demapped into bits. Finally, low-density parity-check (LDPC) decoding is applied to correct any errors, resulting in the final received bit stream.

III. ML-BASED FRAMEWORK FOR PAPR REDUCTION

The proposed ML framework integrates principal component analysis (PCA) with an EN algorithm, referred to in short as EN-PCA. The PCA module serves as the feature extraction method, while the EN algorithm serves as the ML-based scheme for computing the estimated $\widetilde{\mathbf{y}}$, targeting PAPR reduction within the SatCom system.

First, let us start with the RG which is a matrix composed of $M \times N_{OF}$ complex elements, where M is the total number of sub-carriers and N_{OF} is the number of the OFDM symbols. Recall that the RG is structured as a matrix of resource elements, with each physical resource block (PRB) occupying a portion within this grid. Each PRB is a resource block that is composed by a subset of 12 subcarries in the frequency domain and one slot in the time domain. The duration of a slot varies depending on the numerology that defines the subcarrier spacing. In this paper, we utilize 51 PRBs, with a subcarrier spacing equal to 15 kHz, where each slot spans 1 ms and contains 14 OFDM symbols. Then, to manage the high dimension of the RG, especially when it is used as input for the ML model, we apply the PCA as a feature compression technique. Following the PTS method detailed in Section II, we have V subblocks for each column of the RG, leading to a total of $N_{OF} \times V$ columns. For each of the $N_{OF} \times V$ columns, the absolute value of its M elements corresponds to the input of the PCA module for dimension reduction. This process yields a new set of uncorrelated features, N_{PC} (the principal components), allowing the PCA technique to capture the most important patterns in the data. After the feature compression procedure, we obtain the selected features that will serve as the input to the ML model. Consequently, the input dimension of each sample for the ML scheme is given by $N_{PC} \times N_{OF} \times V$.

Meanwhile, the weighting factors are denoted as $\mathbf{W} = [W_1, ..., W_V]$, where $W_v = e^{jy_v} \in \mathbb{C}$, $v = 1, ..., V$. In the case of continuous rotation factors, y_v is constrained within the range $[0, 2\pi)$. Conversely, for discrete phase weighting factors, the set of possible values for y_v is limited by the set ϕ with $y_v \in \phi$, where $\phi = \left\{0, \frac{2\pi}{P_f}, ..., \frac{2\pi}{P_f} p_f, ..., \frac{2\pi}{P_f} P_f - 1\right\}$, $p_f = 0, ..., P_f - 1$ with P_f as the number of possible phase rotation factors. Therefore, true labels of the ML algorithm are given by $\mathbf{y} = [y_1, ..., y_V]$. These values are obtained by applying the PTS technique in an exhaustive search (ES) manner as it is described in Section II. Finally, the dataset to train the ML model can be denoted as $DH = \{\mathbf{z}_1, ..., \mathbf{z}_n, ..., \mathbf{z}_N\}$, where N is the total number of training samples and $\mathbf{z}_n = \{\mathbf{f}_n, \mathbf{y}_n\}$ in which $\mathbf{f}_n$ is the set of features after the PCA module, and $\mathbf{y}_n$ is the set rotation factors obtained by the ES method.

Then, the EN algorithm is implemented as the ML-based technique used to compute the estimated $\widetilde{\mathbf{y}_n}$ aimed to PAPR reduction in the proposed SatCom system. In this sense, the EN algorithm is a regularization technique to reduce the risk of over-fitting in learning models. Thus, the EN algorithm seeks to minimize the sum of squared errors between observed and predicted values, while simultaneously incorporating both the absolute and squared values of the coefficients into the penalty term. In particular, the EN model combines both L1 and L2 regularization in its objective function, with the balance between them being regulated by a parameter, δ, which controls their convex combination [9], as follows:

$$\min_{w} \left(1/2N\right) \times ||f_n w - y_n||_2^2 + \alpha\delta * ||w||_1 + (\alpha(1-\delta)/2) \times ||w||_2^2. \tag{6}$$

where N is the sample size, $\alpha > 0$ applies the L1 regularization to the weights, and w is the vector of coefficients.

For the model evaluation, the 5-fold cross-validation is used to assess the performance of the machine learning model. In this regard, the dataset was split into 80% for training and 20% for testing. To evaluate the model's accuracy, the predicted values were compared with the actual values from the test set, to compute the mean squared error (MSE), mean absolute error (MAE), and root mean square error (RMSE), as shown in Section V.

IV. PSO AIDED PTS-BASED SCHEME FOR PAPR REDUCTION

In this section, we describe the PSO technique as a baseline approach for determining the phase weighting factor vector, W_v, within the PTS framework. This method effectively achieves near-optimal results while maintaining low CC [7]. In this context, PSO contains a population of R_{PSO} particles, where each r-th particle has an associated position $\mathbf{x}_r$, velocity $\mathbf{v}_r$ and fitness value $f(\mathbf{x}_r)$. At each t-th iteration, the position of the particle with the lowest fitness value is designated as the global best position $\mathbf{g}^t$. Meanwhile, each particle retains a local best position $\mathbf{x}_{LB,r}^t$ which represents the highest-performing position reached by that particle up to the t-th iteration.

The position of the particle defines its phase rotation factors. Specifically, the position of the r-th particle is represented by $\mathbf{x}_r = [x_{1,r}, ..., x_{V,r}]$, where V indicates the number of disjoint subblocks. The phase rotation factor for the v-th subblock, determined by the r-th particle, is denoted as $W_{v,r} = e^{jx_{v,r}} \in \mathbb{C}$. For the phase rotation factors, the values of $x_{v,r}$ are restricted to the set ϕ with $x_{v,r} \in \phi$, where $\phi = \left\{0, \frac{2\pi}{P_f}, ..., \frac{2\pi}{P_f} p_f, ..., \frac{2\pi}{P_f} P_f - 1\right\}$, $p_f = 0, ..., P_f - 1$ and P_f is the number of possible phase rotation factors.

Algorithm 1 PSO aided PTS-based framework.

inputs: Number of particles, R_{PSO}, maximum number of iterations, $T_{PSO}^{\max}$, number of sub-blocks, V, define the set ϕ and number of possible phase rotation factors, P_f.
Initialize the iteration counter, $t = 1$.
Initialize each particle's initial position and velocity, r-th particle, and $\mathbf{x}_r^t, \mathbf{v}_r^t$, respectively.
Evaluate the initial PAPR value for each particle position, $f(\mathbf{x}_r^t)$.
Determine the local and global best positions, $\mathbf{x}_{LB,r}^t, \mathbf{g}^t$.
While $t \leq T_{PSO}^{\max}$ **do**
  for $r = 1$ to R_{PSO} **do**
    Calculate the new velocity, $\mathbf{v}_r^{t+1}$, and position, $\mathbf{x}_r^{t+1}$, for each particle, by using equations (7), and (8), respectively.
    Restrict each element of $\mathbf{x}_r^{t+1}$ to the closest value in ϕ for the phase factors.
    Evaluate the PAPR value $f\left(\mathbf{x}_r^{t+1}\right)$.
    Update the local best position:
    if $f\left(\mathbf{x}_r^{t+1}\right) < f\left(\mathbf{x}_r^t\right)$ **then** $\mathbf{x}_{LB,r}^{t+1} = \mathbf{x}_r^{t+1}$
    else $\mathbf{x}_{LB,r}^{t+1} = \mathbf{x}_r^t$
  end for
  Update the global best position: $\mathbf{g}^{t+1} = \underset{1 \leq r \leq R_{PSO}}{\arg\min}\ f\left(\mathbf{x}_{LB,r}^{t+1}\right)$.
  Increase the iteration counter: $t = t + 1$.
end while
output: the best particle position, $\mathbf{g}^t = [g_1^t, ..., g_V^t]$, and assign $\mathbf{W} = \left[e^{jg_1}, ..., e^{jg_V}\right]$ as the phase rotation factors for all subblocks.

The fitness value $f(\mathbf{x}_r)$ for the r-th particle is determined by the PAPR resulting from the phase rotation factors $\mathbf{W}_r = [W_{1,r}, ..., W_{V,r}]$, with $f(\mathbf{x}_r)$ defined as per equation (3).

The PSO-based algorithm begins with initializing the position of each particle, $\mathbf{x}_r^1$, where each position element is randomly chosen from the set ϕ. Following this, the initial velocity of each particle is set to zero, and its subsequent updates are governed by the following equation:

$$\mathbf{v}_r^{t+1} = I_w \mathbf{v}_r^t + c_1 \lambda_1 \left(\mathbf{x}_{LB,r}^t - \mathbf{x}_r^t\right) + c_2 \lambda_2 \left(\mathbf{g}^t - \mathbf{x}_r^t\right), \quad (7)$$

where I_w denotes the inertia weight, λ_1 and λ_2 represent the acceleration parameters, and c_1, c_2 are random numbers within the interval $[0, 1]$. The updated position of each particle is then calculated as follows:

$$\mathbf{x}_n^{t+1} = \mathbf{x}_r^t + \mathbf{v}_r^{t+1}. \quad (8)$$

This process is repeated until the maximum iteration limit, $T_{PSO}^{\max}$, is reached. Additionally, after step (8), each element of the updated position $\mathbf{x}_r^{t+1}$ is mapped to its nearest value within the set ϕ to determine the rotation factors. The procedure for the proposed PSO-based scheme is outlined in Algorithm 1.

V. Simulation Results

In this section, we provide the simulation results programmed into MATLAB and Python software of the swarm intelligence and ML algorithms-aided PTS-based schemes for PAPR reduction. Regarding the swarm intelligence techniques, we present the performance comparison in terms of CCDF, CC, and CT, of the PSO-PTS, ACO-PTS, and QPSO-PTS. In this context, the CCDF metric is defined as the probability of the PAPR exceeding a certain threshold. Furthermore, for the ML models, we present simulation results for the proposed EN-based scheme. and for the RF, ET, and SVR benchmark models. The simulation results are averaged over several frames of 10ms, and 16-QAM modulation is employed following the scheme described in Fig. 1 with the LMS channel model. Moreover, the oversampling factor is equal to L=4. Table I summarizes the main simulation parameters of the proposed network.

TABLE I
Network parameters for the ML-aided PTS scheme

Parameter	Value	Description
$N^{\text{slot}}\text{symb}$	14	Number of OFDM symbols per slot
$N\text{FFT}$	128	FFT size
$f_{\text{cs}}(GHz)$	3.8	Frequency of the carrier signal
Δf (kHz)	15	Subcarrier spacing in Hz
M	16	Modulation order
CP	10	Cyclic prefix length
Channel model	LMS	Channel model type
Speed (m/s)	2	Speed of movement of ground terminal
Delay Spread (ns)	300	Channel delay spread
Rt	$616/1024$	Code rate
δ	5	IBO (dB)

A. Swarm intelligence-based schemes for PAPR reduction

The simulation parameters of each swarm intelligence scheme in Table II are set based on the best performance achieved through several experiments. The variables T_{PSO}^{max}, T_{QPSO}^{max}, and T_{ACO}^{max} denote the number of iterations for PSO, QPSO, and ACO, respectively. In addition, to validate the optimality of the swarm intelligence-based schemes, we consider the ES method for searching the optimal phase factors in the PTS technique.

Fig. 2 shows the convergence behavior of the swarm intelligence-based schemes versus the number of iterations for PAPR reduction with different number of phase rotation

TABLE II
Simulation parameters of swarm intelligent algorithms

Algorithm	Simulation parameters
PSO	Number of iterations, $T_{PSO}^{max} = 80$ Number of particles, $R_{PSO} = 30$ Inertia weight, $Ine = 0.7$ Scalar factors, $c_1, c_2 = 1.494$
QPSO	Number of iterations, $T_{QPSO}^{max} = 100$ Number of particles, $R_{QPSO} = 30$
ACO	Number of iterations, $T_{ACO}^{max} = 100$ Number of particles, $R_{ACO} = 30$ Sample size, $S_{ACO} = 30$

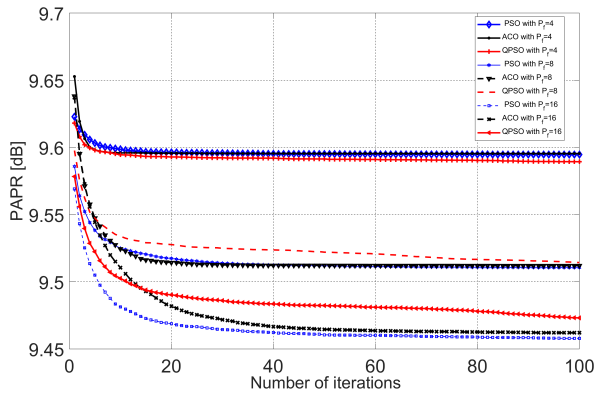

Fig. 2. Convergence behavior of the swarm intelligence-based algorithms

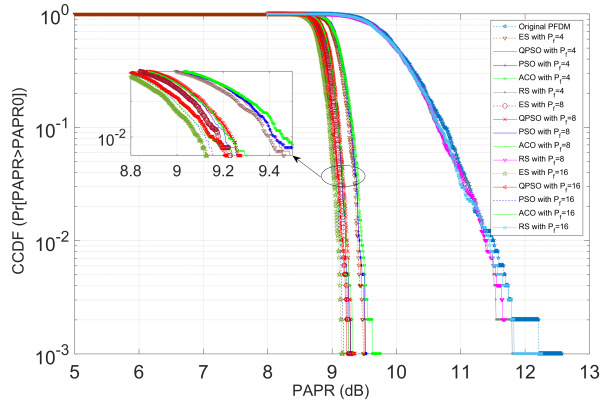

Fig. 3. CCDF Vs. PAPR between the swarm intelligence algorithms-aided the PTS technique and the ES method.

factors, P_t. From Fig. 2, it can be observed that as the number of iteration increases, the PAPR performance of the SIA decreases. Moreover, Fig. 2 shows that the QPSO method achieves a slightly better PAPR reduction compared to the PSO and ACO algorithms. However, when the number of phase rotation factors, P_t, increases, the PSO-based scheme achieves faster convergence than that obtained by both the QPSO and ACO methods.

Fig. 3. shows the CCDF performance between the swarm intelligence-aided PTS-based schemes, random scheme (RS) and the ES method when the phase rotation factors are equal to $P_f = 4$, $P_f = 8$ and $P_f = 16$. In this regard, Fig. 3 validates the results shown in Fig. 2, which demonstrates that as the number of the phase rotation factors, P_f, increases, the CCDF performance improves. Moreover, from Fig. 3, it can be observed that the PSO, ACO, and QPSO methods achieve CCDF values comparable to those of the optimal ES method, while reducing CC.

1) Complexity Analysis: In this subsection, Table III summarizes the CC of the PSO, QPSO, ACO, and the ES methods, where T^{max}_{PSO}, T^{max}_{QPSO}, and T^{max}_{ACO} denote the maximum iteration counts for the PSO, QPSO, and ACO algorithms, respectively. The CT per iteration for PSO, QPSO, and ACO

TABLE III
COMPUTATIONAL COMPLEXITY

Algorithm	Computational Complexity
PSO	$\mathcal{O}\left(T^{max}_{PSO} \times R_{PSO}\right)$
QPSO	$\mathcal{O}\left(T^{max}_{QPSO} \times R_{QPSO}\right)$
ACO	$\mathcal{O}\left(T^{max}_{ACO} \times S_{ACO}\right)$
ES	$\mathcal{O}\left(P_f^{V-1}\right)$

is recorded as 0.8558s, 1.1407s, and 1.2098s, respectively. Furthermore, the CT required by the ES method—used in PTS without SIA for identifying optimal phase rotation factors is 2.45s. The simulations were performed on a computer with 16 GB RAM and an Intel Core i7-10610U CPU.

B. ML-aided PTS for PAPR reduction

In this subsection, we present the simulation results for the ML-based schemes aimed at reducing the PAPR in the proposed SatCom system. In this sense, Table IV provides the simulation parameters of the investigated ML models.

TABLE IV
SIMULATION PARAMETERS OF THE ML-BASED SCHEMES

ML model	Simulation parameters
EN	ElasticNet mixing, $l1_{ratio} = 0.5$ Maximum iterations, $Max_{ite} = 50$ Selection, $s = random$
RF	Number of estimators, $N_{RF} = 200$ Max depth, $Max_d = 10$
ERTR	Number of estimators, $N_{ET} = 200$ Max depth, $Max_{dET} = 10$
SVR	Number of support vectors, $N_{RF} = 200$ Kernel, $ker = rbf$

1) Evaluation with 5-fold cross validation: In this subsection, we assess the performance of the ML regression schemes by applying 5-fold cross-validation [8] to obtain RMSE, MAE, and MSE. Specifically, RMSE is the square root of the average of the squares of the differences between the actual value and the estimated value, MAE is the average relative error [8], which considers the absolute error between predicted value $\widehat{y_v}$ and the real measure, y_v, divided by the real measure. The MSE metric is the simple form of RMSE, which calculate the squares of the differences between the actual value and the estimated value. In this sense, Table V compares the performance in terms of the MSE, MAE, and RMSE error metrics for the EN, RF, ET, SGD, and DNN. From Table V, we can observe that the proposed EN-based model overcomes the other ML baseline schemes. Moreover, we evaluate the CC [9], [8] and CT in Table VI . From Table VI, it can be observed that the EN-based approach outperforms the baseline schemes. Specifically, it is validate that the EN scheme offers significantly lower CT complexity compared to the PSO method.

Fig. 4 shows the CCDF versus the PAPR performance between the PSO technique and the proposed ML framework based on the EN model, when the number of sublock and PCA components are equal to $V = 4$, and $N_PC = 10$, respectively.

TABLE V
PERFORMANCE COMPARISON BETWEEN THE PROPOSED EN-BASED APPROACH AND BASELINE SCHEMES

SNR (dB)	EN	RF	ERTR	SVR
MSE	2.7	2.95	2.9	3.1
MAE	0.00215	0.00315	0.00255	0.00319
RMSE	1.643	1.645	1.644	1.683

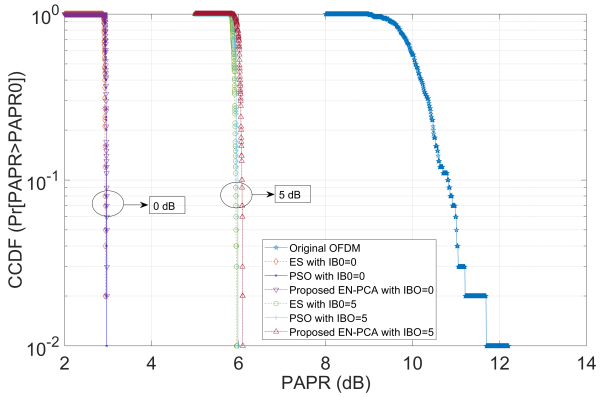

Fig. 4. CCDF Vs. PAPR between the PSO and the EN model.

From Fig. 4, it can be observed that when the IBO is higher, the CCDF performance decrease. This is because, a high IBO delivers a distortion-free output signal, but reduces energy efficiency. Conversely, a low IBO enhances energy efficiency but introduces distortion and interference into the signal [11]. Moreover, from Fig. 4, we can observe that the EN and the PSO technique achieve a comparable CCDF performance obtained by the optimal ES method. However, the CT required by the proposed EN model outperforms both the PSO and ES methods. As shown in Table VI, the EN model achieves a CT of 0.01212s, significantly faster than the 0.8558s required by PSO and the 2.45s by the ES method.

2) Complexity Analysis: Table VI shows the CC of the ML-based schemes. Applying the PCA technique reduces the dimensionality of the feature set used for predicting phase rotation factors, $\widetilde{\mathbf{y}}$. This reduction in feature dimensionality leads to lower CC and processing time, particularly benefiting the EN method, whose complexity relies on the number of features.

TABLE VI
COMPUTATIONAL COMPLEXITY

Algorithm	Computational complexity	Computational time [s]
EN	$O(f)$	0.001212
RF	$O(N_{RF}Max_d)$	0.090999
ERTR	$O(N_{ET}Max_{dET})$	0.080999
SVR	$O(N_{RF}f)$	0.0999
PSO	$\mathcal{O}\left(T_{PSO}^{max} \times N_{PSO}\right)$	0.8558

VI. CONCLUSION

In this paper, we exploit the benefits of low complexity provided by the AI algorithms to reduce the PAPR in SatCom systems where the SIA and the ML techniques are investigated. In particular, we designed a novel ML model-aided PTS framework based on the implementation of the PCA and the EN algorithm. Regarding the SIA, we applied the PSO, the ACO, and the QPSO-based schemes. On the other hand, in the ML domain, we employed the EN, the ERTR, the RF, and the SVR models aided by the PCA technique. These swarm intelligence and ML algorithms were designed to optimize phase rotation factors within the PTS framework, thus reducing CC. Satisfactorily, the proposed ML model based on the PCA and the EN algorithm achieved a near-optimal solution comparable to the ES method but with significantly reduced computational demands. In contrast, the ES method systematically examines all potential solutions within the search space, leading to high complexity as the number of subblocks and phase rotation options increase. Furthermore, while the SIA methods demonstrated performance close to that of ES, the PSO outperformed other swarm intelligence baselines. Nevertheless, the proposed EN-based framework achieved similar performance with even lower computational requirements than the SIA methods. This work demonstrates that AI-driven approaches can offer an efficient, low-complexity solution for PAPR reduction in SatCom, based on ML models, particularly the EN with the PCA technique, standing out for their balance between accuracy and computational efficiency.

REFERENCES

[1] S. M. Eghbali and I. Beiranvand, "PTS OFDM scheme based on ICA algorithm for PAPR reduction in satellite communication," *Indian Journal of Science and Technology*, vol. 8, no. 12, Jun. 2015.

[2] Y. A. Jawhar, L. Audah, M. A. Taher, K. N. Ramli, N. S. M. Shah, M. Musa, and M. S. Ahmed, "A review of partial transmit sequence for papr reduction in the OFDM systems," *IEEE Access*, vol. 7, p. 18021–18041, 2019.

[3] L. Li, L. Xue, X. Chen, and D. Yuan, "Partial transmit sequence based on discrete particle swarm optimization with threshold about PAPR reduction in FBMC/OQAM system," *IET Communications*, vol. 16, p. 142–150, 2021.

[4] M. Hossein Aghdam and A. Sharifi, "A novel ant colony optimization algorithm for PAPR reduction of OFDM signals," *International Journal of Communication Systems*, vol. 34, p. 142–150, 2020.

[5] X. Wang, N. Jin, and J. Wei, "A model-driven DL algorithm for PAPR reduction in OFDM system," *IEEE Communications Letters*, vol. 25, no. 7, p. 2270–2274, Jul. 2021.

[6] A. Kalinov, R. Bychkov, A. Ivanov, A. Osinsky, and D. Yarotsky, "Machine learning-assisted PAPR reduction in massive MIMO," *IEEE Wireless Communications Letters*, vol. 10, no. 3, p. 537–541, Mar. 2021.

[7] M. O. Okwu and L. K. Tartibu, "Metaheuristic optimization: Nature-inspired algorithms swarm and computational intelligence, theory and applications," *Studies in Computational Intelligence*, 2021.

[8] C. E. García and I. Koo, "Extremely randomized trees regressor scheme for mobile network coverage prediction and REM construction," *IEEE Access*, vol. 11, pp. 65 170–65 180, 2023.

[9] A. Gupta, J. Du, D. Chizhik, R. A. Valenzuela, and M. Sellathurai, "Machine learning-based urban canyon path loss prediction using 28 ghz manhattan measurements," *IEEE Transactions on Antennas and Propagation*, vol. 70, no. 6, p. 4096–4111, Jun. 2022.

[10] A. Saleh, "Frequency-independent and frequency-dependent nonlinear models of TWT amplifiers," *IEEE Transactions on Communications*, vol. 29, no. 11, p. 1715–1720, Nov. 1981.

[11] C. H. Azolini Tavares, J. C. Marinello Filho, C. M. Panazio, and T. Abrão, "Input back-off optimization in OFDM systems under ideal pre-distorters," *IEEE Wireless Communications Letters*, vol. 5, no. 5, p. 464–467, Oct. 2016.